Adsorption (2010) 16: 147–153
DOI 10.1007/s10450-010-9207-4

Modeling breakthrough curves of volatile organic compounds on activated carbon fibers

Line Fournel · Pierre Mocho · Ross Brown · Pierre le Cloirec

Received: 18 July 2007 / Accepted: 31 January 2010 / Published online: 10 February 2010

Abstract Granular activated carbon (GAC) and more recently activated carbon fibers (ACF) are used for the treatment of volatile organic compounds (VOC) in industrial processes. The purpose of this study was to investigate the adsorption kinetics of ACF to eliminate VOC from polluted air. This approach is carried out by modeling experimental breakthrough curves with two kinds of models: an equilibrium model and a mass transfer model based on a linear driving force (LDF) in conjunction with the Langmuir equilibrium model. The results show the influence of the intraparticle diffusion on the adsorption kinetics of ACF, in spite of their small fiber diameter. Moreover, external diffusion kinetics is fast because of the influence of the large external surface area of ACF on the VOC mass transfer.

Keywords Adsorption · VOC · Activated carbon fibers · Breakthrough curve · Model

L. Fournel
Laboratoire Génie de l'Environnement Industriel,
Ecole des Mines d'Alès, 6 avenue de Clavières, 30319 Alès Cedex, France

P. Mocho (✉)
Laboratoire Thermique Energétique et Procédés,
Université de Pau et des Pays de l'Adour, Avenue de l'Université, BP 1155, 64013 Pau Cedex, France
e-mail: pierre.mocho@univ-pau.fr

R. Brown
Institut Pluridisciplinaire de Recherche sur l'Environnement et les Matériaux, ECP, 2 avenue Pierre Angor, 64053 Pau Cedex 9, France

P. le Cloirec
UMR 6226, Ecole Nationale Supérieure de Chimie de Rennes, Campus de Beaulieu, Avenue du Général Leclerc, 35700 Rennes, France

Abbreviations

a	External surface area of adsorbent particles per unit adsorbent volume, m^2/m^3
C_i	Bulk-fluid phase concentration of component i, kg/m^3
C_{is}	Fluid phase concentration of component i on the surface of particles, kg/m^3
C_{in}	Inlet bulk-fluid phase concentration of component i, kg/m^3
$\overline{C_i}$	Average concentration of component i in the fluid phase inside the particle, kg/m^3
D_e	Effective intraparticular diffusion coefficient, m^2/s
D_K	Knudsen diffusion, m^2/s
D_m	Molecular diffusivity of the component i in the carrier, m^2/s
D_z	Axial dispersion coefficient, m^2/s
d_f	Fiber diameter, m
K	Langmuir isotherm parameter, m^3/kg
k_f	External diffusion coefficient, m/s
k_p	Intraparticular diffusion parameter, 1/s
L	Column length, m
Pe	Peclet number
$\overline{q_i}$	Average solid phase concentration of component i (amount adsorbed), kg/kg
q_{im}	Langmuir isotherm parameter, kg/kg
q_{is}	Concentration of component i on the surface of the particle, kg/kg
r_f	Fiber radius, m
T	Temperature, K
t	Dimensional time
u	Interstitial velocity of fluid, m/s
Y	Dimensionless axial coordinate
z	Axial coordinate, m
ε	Bed void volume fraction
ε_p	Particle porosity
ρ_p	Density of the adsorbent, kg/m^3

ρ_f Density of the fluid, kg/m^3
τ Dimensionless time

1 Introduction

Volatile organic compounds (VOC) are major air pollutants coming partly from industrial processes. Hydrocarbons in combination with NO_x, in the presence of sunlight, undergo photochemical oxidation, producing a photochemical smog that is environmentally hazardous (Khan and Ghoshal 2000). One way to minimize this harmful effect is to reduce the concentration of the VOC by adsorption on porous carbon (Le Cloirec 1998). The process is generally conducted in two steps, since the saturated material requires regeneration (Brasquet and Le Cloirec 1997; Mocho et al. 1996; Salden and Eigenberge 2001). Activated carbon fiber (ACF) is a novel and fibrous adsorbent, which has been developed by carbonization and activation of organic precursor fibers (Ryu et al. 1998). The advantages of ACF are the smaller fiber diameter (which minimizes diffusion limitations and allows rapid adsorption/desorption kinetics), a sharper pore size distribution and excellent adsorption capacity at low concentration of adsorbates, compared with conventional activated granular/powder carbons (Rong et al. 2002).

The purpose of the present paper is to investigate the adsorption kinetics of ACF (cloth and felt) to remove VOC from polluted air in fixed bed columns.

2 Experimental section

2.1 Adsorbents

The adsorbents examined here were produced by Actitex (Levallois, France). Two kinds of ACF were studied: a cloth (CS 1501) and a felt (FC 1201). The adsorbents were dried at 105 °C during 24 h and then kept in a desiccator until used.

2.2 Adsorbates

The VOC used belong to various families of compounds: alcohols (isopropanol), aromatics (toluene), ketones (acetone, methyl ethyl ketone), esters (ethyl acetate) and halogenated compounds (dichloromethane).

2.3 Method

2.3.1 Fixed bed experiments

The column tests were carried out in a PVC column with an internal diameter of 6.6 cm and a height of 5 mm and 1.64 mm for the felt and the cloth respectively.

The inlet vapour concentration was prepared by injecting the liquid solute in a flow of dry air. The required concentration was obtained by adjusting the air flow and the injection rate. The inlet concentration (C_o) of VOC in the flow stream was 2500 mg/m^3 at a temperature of 20 °C. The concentration of outlet gas was controlled by gas phase chromatography (CPG) with a flame ionization detector (FID).

2.4 Theoretical approach

Physical models representative of the fixed bed column dynamics are the same as those in chromatography. The governing equations can be obtained from differential heat and mass balances of the bulk-fluid phase and the particle phase, respectively, for a given component (Bird et al. 1960). Crittenden and Weber (1978), Ruthven (1984) and Tien (1994) provided a review of the existing mathematical models, available for single component and multicomponent fixed bed adsorption systems. Among the most common approaches, the simplest is neglecting both heat and mass transfer resistances by assuming that equilibrium is instantaneously obtained. However, an accurate prediction of breakthrough curves requires considering the mass transfer kinetics. Because of its simple mathematical form, the linear driving force model (LDF) is commonly used to describe mass transfer kinetics in the solid phase. The mass flux is then related to the difference between the equilibrium surface concentration and the average adsorbed phase concentration. Although the global mass transfer coefficient is often considered as an adjustable parameter, as for the ACF here, some authors attempted to correlate its value with pore and surface diffusion coefficients for a granular adsorbent (Furuya et al. 1996). The pore diffusion coefficient is itself influenced by the pore size distribution. It has been suggested that this parameter should be correlated with molecular diffusion and Knudsen diffusion coefficients (Scott and Dullien 1962).

By electrical analogy, the fluid-solid mass transfer is related to two resistive terms: external resistance, depending on external diffusion of the solute in the film localised on the external surface of the adsorbent; and an intraparticular resistance, influenced by several parameters: interaction of solute with the surface during the adsorption step, diffusion of solute in the pores of the adsorbent, diffusion of the solute on the surface of the pores.

The dynamics of a fixed bed involve transport by axial dispersion in the mobile phase, convective transport in the mobile phase, accumulation in the bed void and accumulation in the adsorbent (Markovska et al. 2001; Chuang et al. 2003; Pré et al. 2002). Equilibrium between the two phases is assumed at the fluid-solid interface.

2.4.1 *Fixed bed adsorption with mass transfer effect—LDF model*

The system considered here is an isothermal adsorption column packed with porous material (GAC or ACF). At time zero, a step change occurs in the concentration of an adsorbate introduced in the flowing stream.

Under the above assumptions, the governing equations and appropriate initial and boundary conditions can be written as follows:

$$u\frac{\partial C_i}{\partial z}+\frac{\partial C_i}{\partial t}+\frac{1-\varepsilon}{\varepsilon}\frac{\partial}{\partial t}(\varepsilon_p\overline{C_i}+\rho_p\overline{q_i})=D_z\frac{\partial^2 C_i}{\partial z^2}, \tag{1}$$

initial condition:

$$t=0, \qquad C_i=0, \tag{2}$$

boundary conditions:

$$z=0, \qquad C_{in}=C_i-\frac{D_z}{u}\frac{\partial C_i}{\partial z}, \tag{3}$$

$$z=L, \qquad \frac{\partial C_i}{\partial z}=0. \tag{4}$$

On introducing the dimensionless coordinates and the Peclet number,

$$Y=\frac{z}{L}, \qquad \tau=\frac{ut}{L}, \qquad Pe=\frac{Lu}{D_z},$$

(1)–(4) become

$$\frac{\partial C_i}{\partial Y}+\frac{\partial C_i}{\partial \tau}+\frac{1-\varepsilon}{\varepsilon}\frac{\partial}{\partial \tau}(\varepsilon_p\overline{C_i}+\rho_p\overline{q_i})=\frac{1}{Pe}\frac{\partial^2 C_i}{\partial z^2}, \tag{5}$$

$$\tau=0, \qquad C_i=0, \qquad Y=0,$$

$$C_{in}=C_i-\frac{1}{Pe}\frac{\partial C_i}{\partial Y}, \qquad Y=1, \qquad \frac{\partial C_i}{\partial Y}=0. \tag{6}$$

The adsorption rate expressed in terms of the film resistance is given by:

$$\frac{\partial \overline{q_i}}{\partial t}=\frac{k_f a}{\rho_p}(C_i-C_{is})=\frac{4k_f}{d_f\rho_p}(C_i-C_{is}). \tag{7}$$

The adsorption rate expression based on the linear driving force (LDF) is:

$$\frac{\partial \overline{q_i}}{\partial t}=D_e a\left(\frac{\partial q_i}{\partial r}\right)_{r=R_p}=k_p(q_{is}-\overline{q_i}), \tag{8}$$

where q_{is} and C_{is} are respectively the adsorbed phase and the fluid phase concentrations at the fluid/solid interface and they are in equilibrium. The thermodynamic equilibrium is modeled here by the Langmuir equation (Langmuir 1918):

$$q_{is}=\frac{q_{im}KC_{is}}{1+KC_{is}}, \tag{9}$$

or

$$C_{is}=\frac{q_{is}}{q_{im}K-Kq_{is}}. \tag{10}$$

Under steady state conditions, the rate of mass transfer of adsorbate from the bulk fluid to the external solid surface balances the net rate of intraparticular diffusion:

$$\frac{4k_f}{d_f\rho_p}(C_i-C_{is})=k_p(q_{is}-\overline{q_i}). \tag{11}$$

Substituting (10) into (11), one obtains:

$$q_{is}-\overline{q_i}=\frac{4k_f}{d_f\rho_p k_p}\left(C_i-\frac{q_{is}}{q_{im}K-Kq_{is}}\right). \tag{12}$$

The pore accumulation term is generally small in comparison with the accumulation in the solid phase, so

$$\frac{\partial}{\partial t}(\varepsilon_p\overline{C_i}+\rho_p\overline{q_i})=\rho_p\frac{\partial \overline{q_i}}{\partial t}=\rho_p k_p(q_{is}-\overline{q_i}). \tag{13}$$

Combining (13) and (12) in dimensionless form yields:

$$\frac{\partial \overline{q_i}}{\partial \tau}=\frac{4k_f L}{ud_f\rho_p}\left(C_i-\frac{q_{is}}{Kq_{im}-Kq_{is}}\right). \tag{14}$$

Differentiation of (12) with respect to τ yields:

$$\frac{\partial q_{is}}{\partial \tau}=\frac{\frac{4k_f L}{ud_f\rho_p}(C_i-\frac{q_{is}}{Kq_{im}-Kq_{is}})+\frac{4k_f}{d_f\rho_p k_p}\frac{\partial C_i}{\partial \tau}}{1+\frac{4k_f}{d_f\rho_p k_p}\frac{Kq_{im}}{(Kq_{im}-Kq_s)^2}}. \tag{15}$$

Substituting (14) into (5) yields:

$$\frac{\partial C_i}{\partial Y}+\frac{\partial C_i}{\partial \tau}+\frac{4(1-\varepsilon)k_f L}{ud_f\varepsilon}\left(C_i-\frac{q_{is}}{Kq_{im}-Kq_{is}}\right)=\frac{1}{Pe}\frac{\partial^2 C_i}{\partial Y^2}. \tag{16}$$

The partial differential equation (16) was transformed into a set of linear equations using an implicit finite volume method. The tridiagonal system obtained and the ordinary differential equation (15) were solved with the LU decomposition method and a fifth-order Runge-Kutta method respectively (Finlayson 1980; Chapra and Canale 2002). The mathematical scheme was implemented in Fortran 90 to simulate the breakthrough curve.

For the ACF, the external and intraparticular diffusion parameters are unknown; k_f and k_p defined in (7) and (8) are used as adjustable parameters in modeling adsorption. The Peclet number is also unknown for the ACF; the axial dispersion coefficient D_z will be assumed to be equal to molecular diffusion D_m.

The kinetics of ACF is considered to be fast, so it could be interesting to test an equilibrium model to study the influence of the intraparticular resistance on the mass transfer kinetics.

Table 1 Main characteristics of ACF

Name	ACTITEX CS 1501	ACTITEX FC 1201
Origin	Viscose	Viscose
Texture	Cloth	Felt
Grammage (g/m^2)	200	150
Fiber diameter (μm)	1.6	1.6
Thickness (mm)	0.41	2–3
Structure	Microporous	Microporous
BET surface (Argon, 77 K) (m^2/g)	1420 ± 10	1340 ± 10
Porous volume (cm^3/g)	0.61	0.68
Microporous volume (cm^3/g)	0.58	0.52
Pore median diameter (Å)	5–8	5–8
Purity of carbon (%)	>99	>99
Density (g/cm^3)	1.01	1.01
Bed void fraction	0.52	0.93

2.4.2 *Fixed bed equilibrium model*

The following assumption is made in this model: the porosity of the adsorbent is directly accessible to the adsorbate at the film-adsorbent interface so that intraparticular diffusion resistance can be neglected. Thus, the uptake of adsorbate is fast and one can assume that the fluid phase and the adsorbent phase are in equilibrium.

There is no concentration gradient across the adsorbent. Thus,

$$\overline{q_i} = \frac{q_{im} K C_{is}}{1 + K C_{is}}, \tag{17}$$

$$\frac{\partial \overline{q_i}}{\partial t} = \frac{K q_{im}}{(1 + K C_{is})^2} \frac{\partial C_{is}}{\partial t}. \tag{18}$$

Substituting (7) into (18), one obtains for the ACF:

$$\frac{\partial C_{is}}{\partial t} = \frac{4 k_f (1 + K C_{is})^2}{\rho_p K q_{im} d_f} (C_i - C_{is}). \tag{19}$$

2.4.3 *Estimation of the fitting error*

The fitting efficiency of each model is evaluated by the root mean square error δ:

$$\delta = \frac{1}{C_{in}} \sqrt{\frac{1}{N} (C_{exp} - C_{mod})^2} \tag{20}$$

where C_{exp} and C_{mod} are the observed and calculated concentrations at breakthrough, respectively, and N is the number measured in each test.

3 Results and discussion

Study of the dynamics of a fixed bed requires knowledge of the parameters in the Langmuir equation. They are deduced from experimental isotherm data and reported in Table 2.

Table 2 summarises the Langmuir model characteristics of VOC adsorption on ACF. The maximum adsorptive capacity at the monolayer level q_{im}, and the Langmuir equilibrium constant K are between 0.19 and 0.51 g/g and 0.6 and 48 m^3/g respectively, demonstrating that these ACF are particularly suitable for adsorbing VOC.

3.1 Study of the breakthrough curves of ACF

The breakthrough curves of ACF for toluene, MEK, dichloromethane, acetone, ethyl acetate and isopropanol are shown in Figs. 1 to 4. Simulation data of each model are summarized in Table 3.

Figures 1 to 4 show that the equilibrium model applied to fitting the breakthrough curves of ACF is not successful except in the case of dichloromethane. So, the kinetics of diffusion of the solute in the pores of the fibers is not instantaneous. This fact can be explained by the pore network of the fibers, practically-limited to micropores. On the other hand, the linear driving force model is in good agreement with the experimental curves except for acetone. This demonstrates that intraparticule transfer is the main step of the adsorption kinetics. Similarly, Cheng et al. (2004) developed a model with pore diffusion and surface diffusion to represent intraparticle transfer. Table 3 shows the values of the mass transfer coefficients for felt and cloth. The magnitude of k_f depends on the flow conditions around the fibers. Because of the difference of bed void, the superficial velocity of the gas in the cloth is greater than in the felt, so, the fluid-solid contact time is smaller in the cloth than in the felt. Thus, k_f is here influenced more by the retention time of the fluid in the bed than by the turbulent mixing of the fluid. Moreover, the intraparticle transfer coefficient of the solute in the felt (k_p) is higher than in the cloth because of the presence of mesopores in this adsorbent.

The ratio of rates of external mass transfer to intraparticle mass transfer is given by the mass Biot number in the Table 3. When this number is large like here (of the or-

Table 2 Langmuir model parameters of ACF (Cloth and Felt)

	Felt			Cloth		
	K (m^3/g)	q_{im} (g/g)	r^2	K (m^3/g)	q_{im} (g/g)	r^2
Toluene	11.9	0.42	0.996	48	0.44	0.766
MEK	5.7	0.33	0.922	8	0.39	0.955
Dichloromethane	0.6	0.35	0.878	0.8	0.36	0.971
Acetone	2	0.19	0.973	2.7	0.21	0.993
Ethyl acetate	4.1	0.38	0.858	4	0.51	0.968
Isopropanol	3.3	0.30	0.910	5.9	0.37	0.970

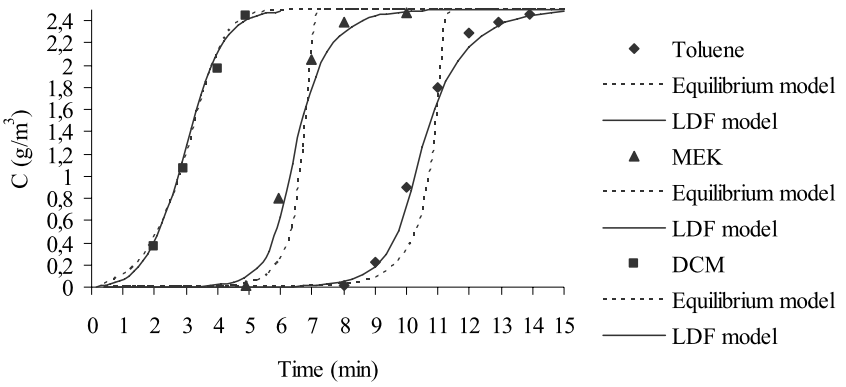

Fig. 1 Breakthrough curve of ACF (Felt) for toluene, MEK and dichloromethane—application of the equilibrium and mass transfer model $C_o = 2.5$ g/m^3, $U_o = 324$ m/h, $L = 5$ mm

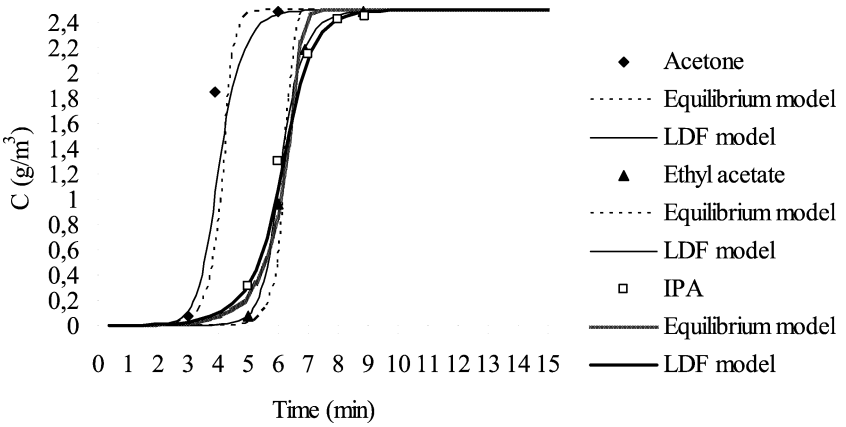

Fig. 2 Breakthrough curve of ACF (Felt) for acetone, ethyl acetate and isopropanol—application of the equilibrium and mass transfer model $C_o = 2.5$ g/m^3, $U_o = 324$ m/h, $L = 5$ mm

der of 10^5), the resistance to the mass transfer is within the fiber rather than external to the fiber. This is in agreement with the failure of the equilibrium model to simulate ACF breakthrough curves. To investigate the intraparticle transfer mechanism, the effective intraparticular diffusion coefficient (D_e) is quantified from the value of k_p; it varies between 3×10^{-15} and 1.5×10^{-14} m^2/s. This very low value leads to the hypothesis that the limiting step of the intraparticle transfer is the diffusion on the internal (pore) surface rather than in the pore volume.

A particularity of the ACF is their fibrous texture with a great surface area a. For example, this parameter is equal to 2.5×10^6 m^2/m^3 for ACF, while it is at most 3000 for a granular activated carbon of 2 mm mean diameter. The surface area has an incidence on the mass transfer rate, which is a function of k_f but also depends of the external surface area and on the driving force. This fact may explain the fast mass transfer rate observed for these materials in spite of the limitation of intraparticule mass transfer. The small diameter of the fiber is also an advantage for the intraparticule mass transfer because of the weak thickness of intraparticle diffusion.

In the case of dichloromethane, the low value of the equilibrium constant K may be related to a low value of the adsorption enthalpy, representing weak adsorbate-adsorbent interaction energy and a low affinity between DCM and ACF. This is consistent with fast establishment of equilibrium and a low adsorption capacity revealed by the fast breakthrough, cf. Fig. 1. The equilibrium model therefore describes this case well.

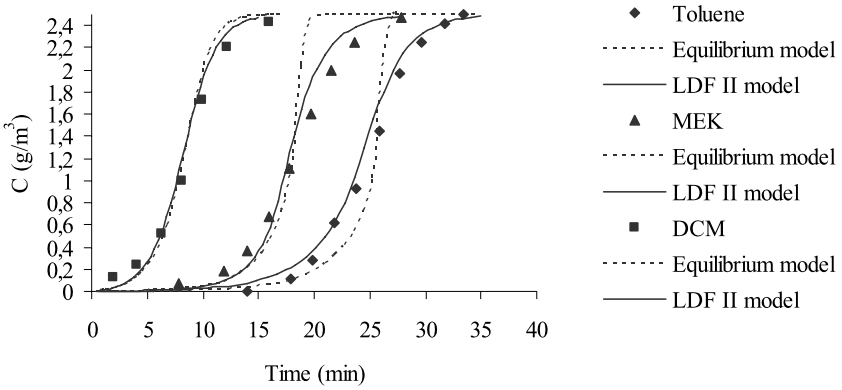

Fig. 3 Breakthrough curve of ACF (Cloth) for toluene, MEK and dichloromethane—application of the equilibrium and mass transfer model $C_o = 2.5$ g/m^3, $U_o = 324$ m/h, $L = 1.64$ mm

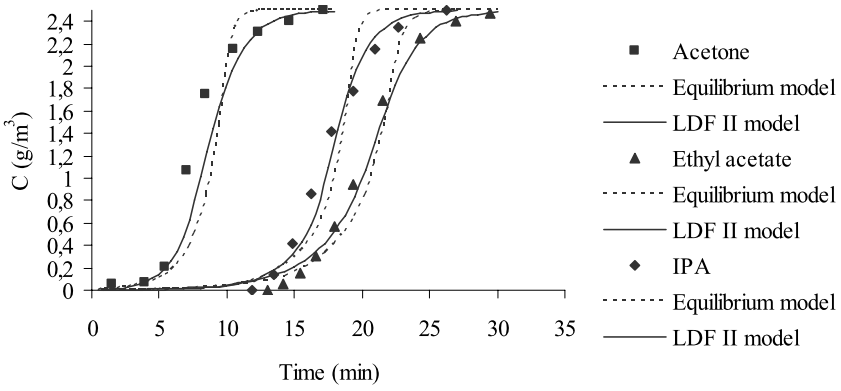

Fig. 4 Breakthrough curve of ACF (Cloth) for acetone, ethyl acetate and isopropanol—application of the equilibrium and mass transfer model $C_o = 2.5$ g/m^3, $U_o = 324$ m/h, $L = 1.64$ mm

Table 3 Parameters of the numerical simulation

Number of finite volume $Nz = 500$ $\Delta\tau/\Delta z = 1$

Compound	Adsorbent	Mass transfer model (LDF)			$D_e \approx \frac{k_p r_f}{a}$	$Bi \approx \frac{k_f r_f}{D_e}$	Equilibrium model	
		k_f (m/s)	k_p (1/s)	δ			k_f (m/s)	δ
Toluene	Cloth	6.66×10^{-4}	10^{-2}	0.02	3.20×10^{-15}	1.67×10^{5}	6.66×10^{-4}	0.1
	Felt	3.33×10^{-3}	1.66×10^{-2}	0.03	5.31×10^{-15}	5.02×10^{5}	3.33×10^{-3}	0.12
MEK	Cloth	6.66×10^{-4}	8.33×10^{-3}	0.05	2.67×10^{-15}	2.00×10^{5}	6.66×10^{-4}	0.14
	Felt	3.33×10^{-3}	2.5×10^{-2}	0.04	8.00×10^{-15}	3.33×10^{5}	3.33×10^{-3}	0.12
DCM	Cloth	8.33×10^{-4}	4.17×10^{-2}	0.03	1.33×10^{-14}	4.99×10^{4}	8.33×10^{-4}	0.04
	Felt	1.66×10^{-3}	8.33×10^{-2}	0.03	2.67×10^{-14}	4.98×10^{4}	1.66×10^{-3}	0.04
Acetone	Cloth	8.33×10^{-4}	1.33×10^{-2}	0.11	4.26×10^{-15}	1.57×10^{5}	5×10^{-4}	0.16
	Felt	6.66×10^{-3}	5×10^{-2}	0.1	1.60×10^{-14}	3.33×10^{5}	3.33×10^{-4}	0.19
Ethyl acetate	Cloth	6.66×10^{-4}	1.33×10^{-2}	0.03	4.26×10^{-15}	1.25×10^{5}	6.66×10^{-4}	0.06
	Felt	6.66×10^{-3}	4.17×10^{-2}	0.02	1.33×10^{-14}	3.99×10^{5}	6.66×10^{-3}	0.11
IPA	Cloth	8.33×10^{-4}	1.33×10^{-2}	0.06	4.26×10^{-15}	1.57×10^{5}	8.33×10^{-4}	0.12
	Felt	1.67×10^{-3}	4.17×10^{-2}	0.04	1.33×10^{-14}	1.00×10^{5}	1.67×10^{-3}	0.1

4 Conclusions

This study deals with the modeling of breakthrough curves of six VOC on two kinds of ACF (cloth and felt). The Langmuir model parameters (K, q_{im}) indicate the good adsorption capacity of ACF to remove VOC. Based on the breakthrough curves modeling, it is concluded that the intraparticular mass transfer is the limitation step of the adsorption kinetics. This is in agreement with the pore structure of ACF, predominantly micropores. The main step of the intraparticule transfer seems to be the surface diffusion, considering the very low effective intraparticular diffusion coefficient (D_e). In the future, a model based on surface diffusion will be developed to validate this assumption.

The successful adaptation of the equilibrium model to dichloromethane breakthrough curves is correlated with the weak adsorbate-adsorbent interaction and the low affinity between DCM and ACF.

References

Bird, R.B., Stewart, W.E., Lightfoot, E.N.: Transport Phenomena. Wiley, New York (1960)

Brasquet, C., Le Cloirec, P.: Adsorption onto activated carbon fibers: application to water and air treatments. Carbon **35**, 1307–1313 (1997)

Chapra, S.C., Canale, R.P.: Numerical Methods for Engineers. McGraw-Hill, New York (2002)

Cheng, T., Jiang, Y., Zhang, Y., Liu, S.: Prediction of breakthrough curves for adsorption in activated carbon in a fixed bed. Carbon **42**(15), 3081–3085 (2004)

Chuang, C.L., Chiang, P.C., Chang, E.E.: Modeling of VOC adsorption onto activated carbon. Chemosphere **53**, 17–27 (2003)

Crittenden, J.C., Weber, W.J.: Predictive model for design of fixed-bed adsorbers: single-component model verification. J. Environ. Eng. **104**(2), 433–443 (1978)

Finlayson, B.A.: Nonlinear Analysis in Chemical Engineering. McGraw-Hill, New York (1980)

Furuya, E.G., Chang, H.T., Miura, Y., Yokomura, H., Tajima, S., Yamashita, S., Noll, K.E.: Intraparticle mass transport mechanism in activated carbon adsorption of phenols. J. Environ. Eng. **122**(10), 909–916 (1996)

Khan, F.K., Ghoshal, A.K.: Removal of volatile organic compounds from polluted air. J. Loss Prevent. Proc. **13**, 527–545 (2000)

Langmuir, L.: The adsorption of gases on plane surface of glass, mica and platinium. J. Am. Chem. Soc. **40**, 1361–1366 (1918)

Le Cloirec, P.: Les Composés Organiques Volatils dans l'Environnement. Lavoisier, Paris (1998)

Markovska, L., Meshko, V., Noveski, V., Marinkovski, M.: Solid diffusion control of the adsorption of basic dyes onto granular activated carbon and natural zeolite in fixed bed columns. J. Serbian Chem. Soc. 463–475 (2001)

Mocho, P., Bourhis, J.C., Le Cloirec, P.: Regeneration of activated carbon loaded with VOC by induction heating. Carbon **34**, 851–856 (1996)

Pré, P., Delage, F., Le Cloirec, P.: A model to predict the adsorber thermal behavior during treatment of volatile organic compounds onto wet activated carbon. Environ. Sci. Technol. **36**, 4681–4688 (2002)

Rong, H., Ryu, Z., Zheng, J., Zhang, Y.: Effect of air oxydation of Rayon-based activated carbon fibers on the adsorption behavior for formaldehyde. Carbon **40**, 2291–2300 (2002)

Ruthven, D.M.: Principles of Adsorption and Adsorption Processes. Wiley, New York (1984)

Ryu, Z., Zheng, J., Wang, M.: Porous structure of pan-based activated carbon fibers. Carbon **36**(4), 427–433 (1998)

Salden, A., Eigenberge, G.: Multifunctional adsorber/reactor concept for waste air purification. Chem. Eng. Sci. **56**, 1605–1611 (2001)

Scott, D.S., Dullien, F.A.L.: Diffusion of ideal gases in capillaries and porous solid. AIChE J. **8**, 113–118 (1962)

Tien, C.: Adsorption Calculations and Modeling. Butterworth-Heinemann, Washington (1994)